Acoustic-phonon propagation in rectangular semiconductor nanowires with elastically dissimilar barriers

E. P. Pokatilov,* D. L. Nika,* and A. A. Balandin†
Nano-Device Laboratory, Department of Electrical Engineering, University of California—Riverside, Riverside, California 92521, USA
(Received 15 February 2005; revised manuscript received 15 August 2005; published 30 September 2005)

We have theoretically studied acoustic phonon spectra and phonon propagation in rectangular nanowires embedded within elastically dissimilar materials. As example systems, we have considered GaN nanowires with AlN and plastic barrier layers. It has been established that the acoustically mismatched barriers dramatically influence the quantized phonon spectrum of the nanowires. The barriers with lower sound velocity compress the phonon energy spectrum and reduce the phonon group velocities in the nanowire. The barriers with higher sound velocity have an opposite effect. The physical origin of this effect is related to redistribution of the elastic deformations in the acoustically mismatched nanowires. In the case of the "acoustically slow" barriers, the elastic deformation waves are squeezed in the barrier layer. The effect predicted for the nanowires embedded with elastically dissimilar materials could be used for reengineering phonon spectrum in nanostructures.

DOI: 10.1103/PhysRevB.72.113311 PACS number(s): 68.65.La, 63.20.Dj, 68.35.Iv, 68.35.Ja

Acoustic phonons play an important role in determining the properties of semiconductors and their heterostructures and nanostructures. In many technologically important semiconductors, acoustic phonons determine the thermal conductivity, contribute to relaxation and recombination of charge carries, and limit the charge carrier mobility. In nanostructures with the feature size W smaller then the phonon mean-free path (MFP) Λ_p, the quantization of spatially confined acoustic phonons influences the electron-phonon scattering rates.[1–5] The modification of the acoustic phonon dispersion in semiconductor superlattices has been mostly studied, both experimentally[6] and theoretically, using the elastic continuum model.[7]

There has been very limited work done on the phonon confinement effects in nanowires with the inclusion of the effect of the nanowire barriers. Mingo and Yang[8] reported results of the atomistic study of phonon transport in Si nanowires coated with amorphous material using the Green's function method. Here we use a completely different, elastic continuum, approach to investigate rectangular nanowires embedded into acoustically mismatched, i.e., elastically dissimilar, materials. We demonstrate numerically that the acoustically mismatched barriers dramatically influence the quantized phonon spectrum of the nanowires.

The acoustic hardness of the material is characterized by the acoustic impedance $\zeta=\rho V_s$, where ρ is the mass density of the material and V_s is the sound velocity in a given material. In this paper, as example material systems, we consider the GaN nanowire and two very different types of the barrier materials. The first is commonly used AlN, and the second is plastic. The acoustic impedance mismatch between GaN and plastic is very large $\zeta(\mathrm{GaN})/\zeta(plastic)\approx 25$. It is smaller for the GaN/AlN interface, e.g., $\zeta(\mathrm{GaN})/\zeta(\mathrm{AlN})\approx 1.3$ for the transverse acoustic (TA) phonon modes. The sound velocity V_s has been used as another parameter to characterize the effects of the boundaries. Thus, in the discussion to follow, we will use the following terminology: "acoustically soft" for the material with small ζ and "acoustically slow" for the material with small V_s.

We consider a generic rectangular nanowire, which forms a potential quantum well, confined in a rectangular barrier shell. It is assumed that GaN crystal lattice has a wurtzite structure with reference axis c along the nanowire axis. The axis X_3 of the Cartesian coordinate system is directed along the c axis, while axis X_1 and axis X_2 are in the cross-sectional plane of the nanowire, parallel to its sides (see insets to Fig. 1). The origin of the coordinate system is in the center of the nanowire. The lateral dimensions of the rectangular nanowire itself are denoted by $d_1^{(1)}$ and $d_2^{(1)}$, while the total lateral dimensions (nanowire thickness plus barrier thickness) are d_1 and d_2, correspondingly. For comparison, we calculate the phonon dispersion for both types of nanowires: with and without barrier layers.

The equation of motion for elastic vibrations in an anisotropic medium can be written as

$$\rho\frac{\partial^2 U_m}{\partial^2 t}=\frac{\partial\sigma_{mi}}{\partial x_i}, \tag{1}$$

where $U=(U_1,U_2,U_3)$ is the displacement vector, ρ is the mass density of the material, σ_{mi} is the elastic stress tensor given by $\sigma_{mi}=c_{mikj}U_{kj}$, and $U_{kj}=(1/2)[(\partial U_k/\partial x_j)+(\partial U_i/\partial x_k)]$ is the strain tensor. The normal acoustic phonon modes in an isotropic rectangular quantum wire without the barrier shell ($c_{iklm}=const$) have been studied in Ref. 9 and, for the cubic crystal rectangular quantum wire, by Nishiguchi *et al.*[10] It has been established that for the rectangular nanowire without barrier layers, the general solutions can be written in the form of the power series $(x_1/d_1)^n(x_2/d_2)^m$. When a nanowire with barriers is studied, one has to take into account the fact that the investigated structure is inhomogeneous in the cross-sectional plane of the wire (X_1,X_2). The latter affects the calculation of derivatives in Eq. (1) since the elastic modulus $c_{mikj}(x_1,x_2)$ and the mass density of the material $\rho(x_1,x_2)$ are the piece wise functions of x_1,x_2.

We have used the standard system of the two-index notations. In the wurtzite crystals of hexagonal symmetry (space group C_{6v}^4), there are five different elastic modules: c_{11}, c_{33},

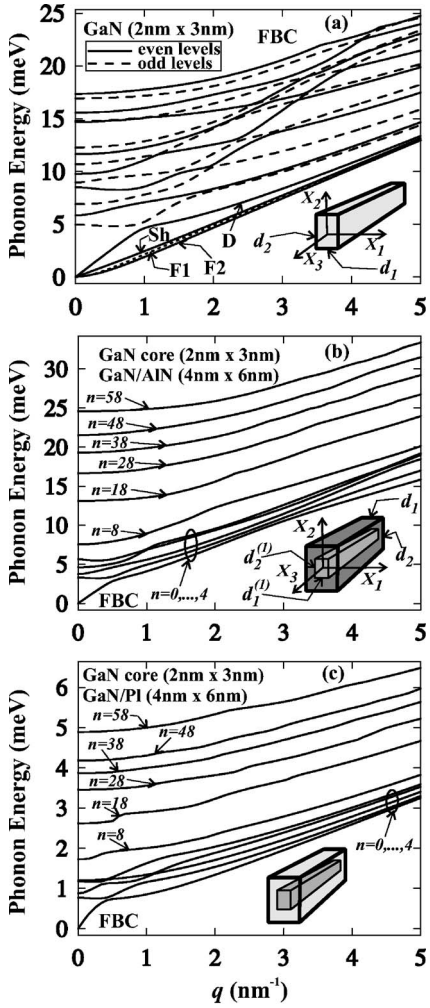

FIG. 1. Phonon dispersion for the dilatational modes for the free-surface boundary conditions at the external barrier boundary. The results are shown for (a) GaN nanowire of the 2 nm×3 nm cross section without the barriers; (b) GaN nanowire with acoustically fast AlN barriers of the 4 nm×6 nm and 2 nm×3 nm GaN nanowire cross sections; and (c) GaN nanowire with acoustically slow barriers of the 4 nm×6 nm and 2 nm×3 nm GaN nanowire cross sections. Note that in panel (a), in addition to the dilatational polarization, all other polarizations such as flexural (F1 and F2) and shear (Sh) are also shown for the ground level $n=0$.

c_{12}, c_{13}, and c_{44}, which are related to each other through the following equalities $c_{11}=c_{1111}=c_{2222}$, $c_{33}=c_{3333}$, $c_{12}=c_{1122}=c_{2211}$, $c_{13}=c_{1133}=c_{3311}=c_{2233}=c_{3322}$, $c_{44}=c_{1313}=c_{3131}$, $c_{55}=c_{44}$, $c_{66}=c_{1212}=c_{2121}=(c_{11}-c_{22})/2$. We have solved Eq. (1) using the approach outlined in Refs. 11 and 12.

The considered structure has two distinctively different symmetry planes and four possible types of the propagating phonon waves, which are the solutions of the elasticity equation.[10] These solutions can be denoted as dilatational (D): $u_1^{AS}(x_1,x_2), u_2^{SA}(x_1,x_2), u_3^{SS}(x_1,x_2) \rightarrow u_i^{D}$; flexural type I (F1): $u_1^{AA}(x_1,x_2), u_2^{SS}(x_1,x_2), u_3^{SA}(x_1,x_2) \rightarrow u_i^{F_1}$; flexural type II (F2): $u_1^{SS}(x_1,x_2), u_2^{AA}(x_1,x_2), u_3^{AS}(x_1,x_2) \rightarrow u_i^{F_2}$; and shear (Sh): $u_1^{SA}(x_1,x_2), u_2^{AS}(x_1,x_2), u_3^{AA}(x_1,x_2) \rightarrow u_i^{Sh}$. Here *SA* and *AS* (symmetric and asymmetric) indicate whether the mode is even or odd with respect of the operation of the sign conversion of the corresponding variable, i.e., $f(x_1,x_2)=f(-x_1,x_2)=f(x_1,-x_2) \rightarrow f^{SS}(x_1,x_2)$, etc.

The outside boundaries of the nanowire, i.e., outside surfaces of the barrier shell, can be either clamped or free. In the case of the clamped boundaries, the boundary conditions on the outside surfaces of the nanowire barrier shell have the form $w_1=w_2=w_3=0$, while in the case of the free boundaries $P_1=P_2=P_3=0$, where $P_i=\sigma_{ik}n_k$ is the force component and n_k is the component of the unitary vector normal to the outer surface. The solutions of Eq. (1) with the given boundary conditions have been found numerically using the finite-difference method. We obtained the phonon dispersion relations for all four types of the phonon polarizations with both free and clamped external boundary conditions for the barrier layers. The calculations were carried out for the nanowires with the cross section 2 nm×3 nm embedded within acoustically slow barrier material and acoustically fast barrier material. The complete cross sections of the nanowire with the barrier layers were 4 nm×6 nm and 6 nm×9 nm. To better elucidate the phonon redistribution effects in the nanowire coated with the acoustically mismatched barrier layer, as an example of the acoustically soft and acoustically slow $[V_s(\mathrm{GaN})/V_s(\mathrm{plastic}) \approx 4]$ material, we have used plastic. The unconventional choice of the material system for the barrier is entirely to better elucidate the phonon spectrum modification and the phonon depletion effect. Other materials systems with small ζ and V_s will lead to similar results. Practical examples of heterostructures with large acoustic impedance and sound velocity mismatch, such as organic-inorganic heterostructures are available.[13–15] A different type of the barrier material considered in this work is AlN. AlN is slightly acoustically softer than GaN$[\zeta(\mathrm{GaN})/\zeta(\mathrm{AlN}) \approx 1.3]$. At the same time, AlN has much higher sound velocity, e.g., $V_s(\mathrm{AlN})/V_s(\mathrm{GaN}) \approx 1.5(1.3)$ for the transverse (longitudinal) phonon modes. In order to investigate the effect of the barrier shells on the phonon spectrum, we also calculated phonon dispersion in the nanowires without barriers, which have cross sections of 2 nm×3 nm in one case and 4 nm×6 nm or 6 nm×9 nm in another case. The values of the elastic constants used in the calculations were taken from Refs. 11 and 16.

Due to a large number of phonon branches of all polarizations present in the rectangular nanowire, we mostly focus on the dilatation polarization branches. In Figs. 1 and 2, we present the plots of the phonon dispersion for the dilatational polarization in the "bare" GaN nanowire of 2 nm×3 nm cross section [Fig. 1(a)], 4 nm×6 nm cross section [Fig. 2(a)], GaN nanowire with AlN barriers of the 4 nm×6 nm and 2 nm×3 nm nanowire cross sections [Fig. 1(b), Fig. 2(b)], GaN nanowire with plastic barriers of the 4 nm×6 nm and 2 nm×3 nm nanowire cross sections [Fig. 1(c), Fig. 2(c)]. Note that Fig. 1(a) shows the lowest phonon modes for all four polarization types: F1, F2, D, and Sh. For the GaN wire of the 2 nm×3 nm cross section, one has $n_{\max}=15$ phonon branches $\omega_n^{(\alpha)}(q)$ of each polarization. In the nanowires of the 4 nm×6 nm cross section, the number of branches of each polarization is already equal to 59, while in the nanowires of the 6 nm×9 nm cross section, this number increases to 135. Since the lattice constants for GaN and

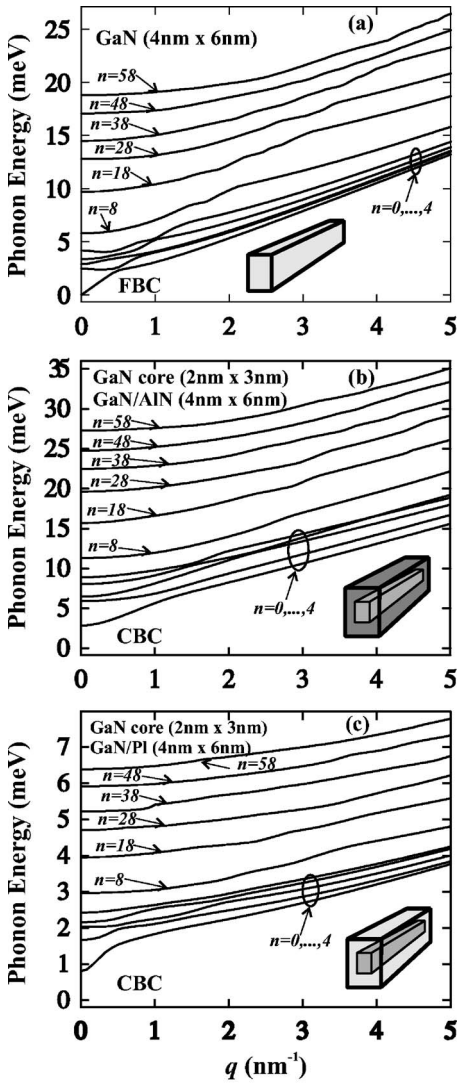

FIG. 2. Phonon dispersion for the dilatational modes for the clamped-surface (b), (c) and free-surface (a) boundary conditions at the external barrier boundary. The results are shown for (a) GaN nanowire of the 4 nm $\times$ 6 nm cross section without the barriers; (b) GaN nanowire with acoustically fast AlN barriers of the 4 nm $\times$ 6 nm and 2 nm $\times$ 3 nm GaN nanowire cross sections; and (c) GaN nanowire with acoustically slow barriers of the 4 nm $\times$ 6 nm and 2 nm $\times$ 3 nm GaN nanowire cross section.

AlN are similar, i.e., $a(\mathrm{GaN})=0.318$ nm, while $a(\mathrm{AlN})=0.311$ nm, the calculation of $n_{\max}=(d_1 d_2)/4a^2$ for the nanowire with either GaN or AlN lattice constants gives approximately the same result. In Figs. 1(b), 1(c), 2(b), and 2(c), we depict the five lowest phonon branches and the higher branches with numbers 8, 18, 28, 38, 48, and $n_{\max}=58$.

The phonon dispersions in Fig. 2(b) and 2(c) are plotted for the clamped boundary conditions (CBC) at the outside surface of the barrier layers. The rest of the curves are plotted for the free-surface boundary conditions (FBC) at the outside surface of the barrier layers. In the case of the clamped outside boundaries [Fig. 2(b) and 2(c)] the bulk-like phonon branches are absent in the phonon spectra, and all phonon energy levels are size quantized. In both free-surface and clamped-surface cases, the difference in the sound velocities of the nanowire and the barrier materials considerably influence the low-energy part of the phonon spectra. The cross-section area of the nanowire also exerts a significant effect. As one can see from the comparison of the plots in Figs. 1(a)–1(c) and Figs. 2(a)–2(c), the change of the outside boundary conditions from the free surface to the clamped surface and the reduction of the cross-section area lead to enhancement of the size quantization in the low-energy part of the phonon spectrum but only weakly influence the high-energy branches. The latter can be explained by the fact that the position of the high-energy levels is mostly determined by the inverse of the lattice parameter $1/a$, whereas the dimensional quantization in the low-energy part of the spectrum depends on $1/d$.

The influence of the elastic properties of the barrier shells is seen very well in the dilatational phonon spectra of the embedded nanowires. The acoustically soft and slow barrier layers lead to the increased density of the phonon branches per energy interval while the acoustically fast barrier layers lead to the density decrease. In the nanowire of the 4 nm $\times$ 6 nm cross section, the energy interval of 6 meV (see Fig. 2(a)) includes the first nine branches, while the energy interval of 18 meV includes all calculated spectrum for $\omega(k=0)$. In comparison with generic slabs, i.e., thin films, the phonon spectrum of nanowires with and without barrier layers is characterized by a larger number of branches $n_{\max}$ due to the spatial confinement in two lateral directions and lower density of phonon branches per unit energy interval. The described strong dependence of the acoustic phonon spectrum on the barrier shell material can be used to tune phonon spectrum and change the phonon-electron scattering rates.

The acoustic phonon group velocity plays an important role in the semiconductor thermal conductivity. Let us analyze how the barrier shells of the rectangular nanowires influence the phonon group velocity. The average frequency-dependent phonon group velocity is calculated using the following definition:

$$\bar{v}(\omega)=\frac{1}{4}\sum_{\alpha}\frac{g^{\alpha}(\omega)}{\sum_{n(\omega)}[v_n^{\alpha}(\omega)]^{-1}}. \tag{2}$$

Here the summation is carried out over all dispersion branches $n(\omega)$ contained in the frequency interval ω, and $g^{(\alpha)}(\omega)$ is the number of the phonon branches. Figure 3 presents the phonon group velocities averaged over all branches from $n=0$ to $n_{\max}$ and over all polarizations types for nanowires with the free-surface boundaries at the outside surface of the barrier layers. The group velocity curves $\bar{v}(\omega)$ are strongly oscillating functions due to the presence of many quantized phonon branches $n(\omega)$ and the fast variation of the derivatives $v_n^{(\alpha)}(\omega)^{-1}=[dq_n^{(\alpha)}(\omega)]/(d\omega)$ with ω. One can see in Fig. 3 that the presence of the acoustically soft and slow plastic barriers has led to a strong reduction of the phonon velocity in the GaN nanowires of the 2 nm $\times$ 3 nm and 4 nm $\times$ 6 nm cross sections in comparison with GaN nanowires without barriers. The presence of AlN barriers, characterized by the high sound velocity, leads to an opposite effect of increasing the phonon group velocity in the nanowire (see Fig. 3).

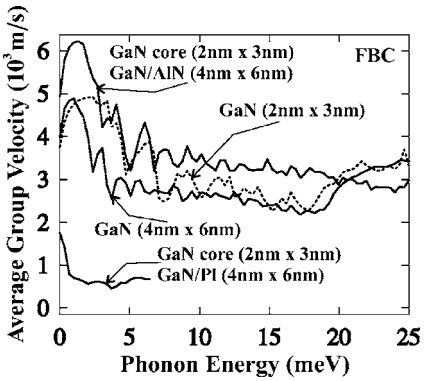

FIG. 3. Polarization and mode averaged phonon group velocities as the function of the phonon frequencies for different GaN nanowires with the free-surface outside boundaries.

It is important to point out that simple averaging of the elasticity modules and mass densities in the considered nanowires with the barrier layers, like it is done in the effective medium approximations, would not have led to such velocity dependence on the barrier structure. The physics of the effect can be elucidated by considering the distribution of the displacements $w(x_1,x_2,q)$ in the cross-sectional plane of the nanowire with acoustically mismatched barrier layers. Figure 4(a) shows the distribution of the dilatational components $w^{(D)}_{3,n=10}(x_1,x_2,q=0.4\ \mathrm{nm}^{-1})$ in the nanowire cross section. Figure 4(b) shows the distribution of $w^{(D)}_{\perp,n=10}(x_1,x_2,q=0.4\ \mathrm{nm}^{-1})$ of the same dilatational mode. One can see from these figures that the displacement vectors of a given mode are concentrated mainly in the acoustically slow barrier shell of the nanowire. The phonon depletion in the acoustically hard material is reinforced in the coated nanowires, compared to thin films,[17] due to spatial confinement along the two lateral directions.

In summary, we have studied acoustic phonon spectra and phonon propagation in rectangular nanowires embedded within elastically dissimilar materials. It has been established that the acoustically mismatched barriers influence the quantized phonon spectrum of the quantum wires. Modification of the acoustic phonon dispersion in the nanowires embedded

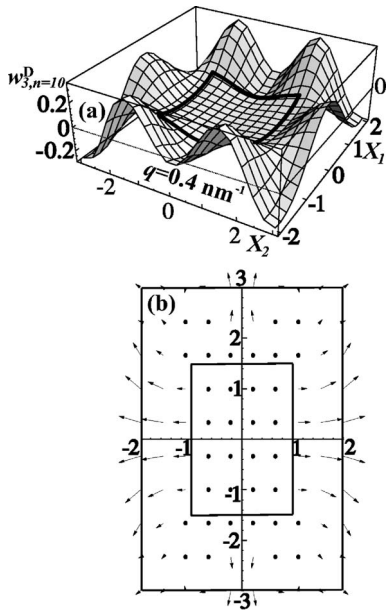

FIG. 4. Distribution of the displacement vector components in the cross-sectional plane of the free-standing GaN nanowire with the acoustically slow barrier layers. The total cross section of the nanostructure is 4 nm$\times$6 nm, the cross section of the nanowire core is 2 nm$\times$3 nm. The results are shown for (a) $w^{(D)}_{3,n=10}\times(x_1,x_2,q=0.4)$ and (b) $w^{(D)}_{\perp,n=10}(x_1,x_2,q=0.4)$.

within the elastically dissimilar materials could be used for reengineering of the phonon spectrum and enhancement of the thermal and charge carrier transport in nanodevices. The acoustic impedance and sound velocity mismatch at the nanowire-barrier interface can become important tuning parameters for phonon engineering.

ACKNOWLEDGMENTS

This work was supported in part by ONR and by DARPA-SRC Microelectronics Advanced Research Corporation (MARCO) and its FENA Focus Center. E. P. P and A. A. B. acknowledge U.S. CRDF support (Project No. MOE2-3057-CS-03). D. L. N's. work was also supported in part by Project No. CRDF-MRDA MTFP-04-06.

*On leave from the Department of Theoretical Physics, State University of Moldova, Kishinev, Republic of Moldova.
†Corresponding author. Electronic address: balandin@ee.ucr.edu

[1] N. Bannov, V. Aristov, V. Mitin, and M. A. Stroscio, Phys. Rev. B **51**, 9930 (1995).
[2] A. Svizhenko, A. Balandin, S. Bandyopadhyay, and M. A. Stroscio, Phys. Rev. B **57**, 4687 (1998).
[3] B. A. Glavin, V. I. Pipa, V. V. Mitin, and M. A. Stroscio, Phys. Rev. B **65**, 205315 (2002).
[4] F. T. Vasko and V. V. Mitin, Phys. Rev. B **52**, 1500 (1995).
[5] N. Nishiguchi, Physica E (Amsterdam), **13**, 1 (2002).
[6] C. Colvard, T. A. Gant, M. V. Klein, R. Merlin, R. Fischer, H. Morkoc, and A. C. Gossard, Phys. Rev. B **31**, 2080 (1985).
[7] S. M. Rytov, Akust. Zh., **2**, 71 (1956) [Sov. Phys. Acoust. **2**, 67 (1956)].
[8] N. Mingo and L. Yang, Phys. Rev. B **68**, 245406 (2003).
[9] *Physical Acoustic*, edited by W. P. Meson (Academic Press, New York, 1964), Vol. I, pt. A.
[10] N. Nishiguchi, Y. Ando, and M. Wybourne, J. Phys.: Condens. Matter **9**, 5751 (1997).
[11] E. P. Pokatilov, D. L. Nika, and A. A. Balandin, Superlattices Microstruct. **33**, 155 (2003).
[12] E. P. Pokatilov, D. L. Nika, and A. A. Balandin, J. Appl. Phys. **95**, 5626 (2004).
[13] X. Yang and X. Xu, Appl. Phys. Lett. **77**, 797 (2000).
[14] Y. Wenge, X. Zheng, T. Feng *et al.*, Displays, **25**, 61 (2004).
[15] P. Urbach, F. Felbier, A. Sorensen, and W. Kowalsky, Jpn. J. Appl. Phys., Part 1 **37**, 1660 (1998).
[16] I. Vurgaftman, J. R. Meyer, and L. R. Ram-Mohan, J. Appl. Phys. **89**, 5815 (2001).
[17] E. P. Pokatilov, D. L. Nika, and A. A. Balandin, Appl. Phys. Lett. **85**, 825 (2004).